J. Fluid Mech. (1988), *vol.* 192, *pp.* 485–509
Printed in Great Britain

Linearized dynamics of two-dimensional bubbly and cavitating flows over slender surfaces

By LUCA D'AGOSTINO, CHRISTOPHER E. BRENNEN AND ALLAN J. ACOSTA
California Institute of Technology, Pasadena, CA 91125, USA

(Received 29 October 1986 and in revised form 23 October 1987)

The present work investigates the dynamics of two-dimensional, steady bubbly flows over a surface and inside a symmetric channel with sinusoidal profiles. Bubble dynamics effects are included. The equations of motion for the average flow and the bubble radius are linearized and a closed-form solution is obtained. Energy dissipation due to viscous, thermal and liquid compressibility effects in the dynamics of the bubbles is included, while the relative motion of the two phases and viscous effects at the flow boundaries are neglected. The results are then generalized by means of Fourier synthesis to the case of surfaces with slender profiles of arbitrary shape. The flows display various flow regimes (subsonic, supersonic and super-resonant) with different properties according to the value of the relevant flow parameters. Examples are discussed in order to show the effects of the inclusion of the various energy dissipation mechanisms on the flows subject to harmonic excitation. Finally the results for a flow over a surface with a Gaussian-shaped bump are presented and the most important limitations of the theory are briefly discussed.

1. Introduction

This paper represents part of a study of the role of the dynamics of bubble volume changes in the fluid mechanics of bubbly or cavitating flows. Specifically, it investigates the effects of the inclusion of the bubble dynamic response in two-dimensional steady flows over surfaces with slender profiles. One of the practical objectives of this study is a better understanding of the global effects of many bubbles in cavitating flows. Traditionally bubbly cavitating flows have been analysed starting with a calculated or measured pressure distribution from the non-cavitating or single-phase flow around, say, a hydrofoil. This is then applied as a known input to the Rayleigh–Plesset equation in order to calculate the bubble volume as a function of position along a streamline. This traditional approach neglects the interactive effect which the bubble growth may have on the pressure distribution, an effect that will increase in magnitude with the number and the extent of the bubbles. While the traditional approach may have validity close to cavitation inception when only an occasional bubble occurs, it clearly loses validity as the cavitation becomes more extensive. Significant alterations will occur in the pressure distribution and in the geometry of the region of cavitation. In water-tunnel tests Gates (1977) observed that laminar separation of the boundary layer on a hemispherical-nosed body was delayed and ultimately eliminated by increasing the number of small bubbles or nuclei present. Moreover, separate tests in which the free-stream velocity was varied suggest that the above phenomenon was not caused by

the 'turbulence' produced by the bubbles. Rather the observations suggest that the bubbles alter the pressure distribution in such a way as to delay separation. These observations have critical consequences for cavitation inception estimations because of the intimate relation between the cavitation inception number and the coefficient of pressure at the laminar separation point (Arakeri & Acosta 1973). More recent experimental observations by Arakeri & Shanmuganathan (1985) and M. Billet (1986, personal communication) have also helped identify the bubble interaction effects in cavitating flows. The photograph and acoustic measurements of Arakeri & Shanmuganathan clearly demonstrate that increasing the number of bubbles decreases their growth and results in a decline of the noise produced per bubble.

One of the objectives of this paper is to provide some guidance as to the nature of these alterations. Despite the extensive linearizations inherent in the analysis we believe that the results convey some qualitative understanding of the nature of the changes that occur in a real cavitating flow.

The last few decades have seen extensive research on the dynamics of bubbly flows (van Wijngaarden 1968, 1972). Early studies based on space-averaged equations for the mixture in the absence of relative motion between the two phases (Tangren, Dodge & Seifert 1949) do not consider bubble dynamic effects. This approach simply leads to an equivalent compressible homogeneous medium. In a classic paper Foldy (1945) accounted for the dynamics of individual bubbles treating them as randomly distributed point scatterers. Assuming that the system is ergodic, the collective effect of bubble dynamic response on the flow is then obtained by taking the ensemble average over all possible configurations. An alternative way to account for bubble dynamic effects is to include the Rayleigh–Plesset equation in the space-averaged equations. Both methods have been successfully applied to describe the propagation of one-dimensional disturbances through liquids containing small gas bubbles (Carstensen & Foldy 1947; Fox, Curley & Larson 1955; Macpherson 1957; Silberman 1957).

However, because of their complexity, there are few reported examples of the application to specific flow geometries of the space-averaged equations that include the effects of bubble response (van Wijngaarden 1964). One exception is the shock wave in a bubbly medium. A number of authors have studied this one-dimensional and time-independent (or slowly varying) flow; a good review of the current state of knowledge of bubble dynamic effects on the structure and evolution of shock waves can be found in Noordzij (1973). Noordzij & van Wijngaarden (1974) have shown that the additional inclusion of relative motion between the bubbles and the liquid can lead to some interesting evolutionary effects and permanent wave solutions. However in the present programme we focus attention on one- or two-dimensional time-dependent flows. In two earlier notes (d'Agostino & Brennen 1983; d'Agostino, Brennen & Acosta 1984) we considered the one-dimensional time-dependent linearized dynamics of a spherical cloud of bubbles subject to an harmonic pressure field and the two-dimensional steady flow of a bubbly liquid over wave-shaped surfaces. The results clearly show that the fluid motion can be critically controlled by bubble dynamic effects. Specifically, the dominating phenomenon consists of the combined response of the bubbles to the pressure in the surrounding liquid, which results in volume changes leading to a global accelerating velocity field. Associated with this velocity field is a pressure gradient which in turn determines the pressure encountered by each individual bubble in the mixture. Furthermore, it can be shown that such global interactions usually dominate any local pressure perturbations experienced by one bubble due to the growth or collapse of a neighbour (see §7).

In the present work the same approach, generalized with the inclusion of dissipative effects in the dynamics of the bubbles, is first applied to steady two-dimensional flows over wave-shaped surfaces (for which there exist well-established solutions for the compressible and incompressible cases) and then is extended to the case of arbitrarily shaped surfaces with slender profiles. Despite all its intrinsic limitations, the following linear analysis indicates some of the fundamental phenomena involved and represents a useful basis for the study of such flows with nonlinear bubble dynamics, which we intend to discuss in a later publication.

2. Basic equations

Following the same approach as previously indicated in our earlier notes (d'Agostino & Brennen 1983; d'Agostino *et al.* 1984), several simplifying assumptions are introduced to obtain a soluble set of equations which still reflects the effects of bubble dynamic response. The relative motion of the two phases is neglected, although its inclusion is also possible (the limitations this imposes are discussed in §7). The liquid is assumed inviscid and incompressible, with density ρ and constant concentration β of bubbles per unit liquid volume. Also, the mass of the dispersed phase and all damping mechanisms in the dynamics of the bubbles are initially neglected. The effects introduced by the inclusion of the liquid viscosity and compressibility on the energy dissipation in the dynamics of the bubbles will be considered later. Then, if external body forces are unimportant, the velocity $\boldsymbol{v}(\boldsymbol{x})$ and the pressure $p(\boldsymbol{x})$ (defined as the corresponding quantities in the liquid in the absence of local perturbations due to any neighbouring bubbles), satisfy the continuity and momentum equations in the form:

$$\nabla \cdot \boldsymbol{v} = \frac{\beta}{1+\beta\tau} \frac{\mathrm{D}\tau}{\mathrm{D}t}, \tag{1}$$

$$\rho \frac{\mathrm{D}\boldsymbol{v}}{\mathrm{D}t} = -(1+\beta\tau)\nabla p, \tag{2}$$

where $\mathrm{D}/\mathrm{D}t$ indicates the Lagrangian derivative, $\tau(\boldsymbol{x})$ is the individual bubble volume and β is related to the void fraction α by: $\beta\tau = \alpha/(1-\alpha)$. Finally, under the additional hypothesis that the bubbles remain spherical, it follows that $\tau = \frac{4}{3}\pi R^3$, with the bubble radius $R(\boldsymbol{x})$ determined by the Rayleigh–Plesset equation (Plesset & Properetti 1977; Knapp, Daily & Hammit 1970):

$$\frac{p_{\mathrm{B}}-p}{\rho} = R\frac{\mathrm{D}^2R}{\mathrm{D}t^2} + \frac{3}{2}\left(\frac{\mathrm{D}R}{\mathrm{D}t}\right)^2 + \frac{2S}{\rho R}. \tag{3}$$

Here S is the surface tension and p_{B} is the bubble internal pressure, which consists of the partial pressures of the vapour p_{v} and non-condensable gas p_{G}. Neglecting thermal and mass diffusion effects within the bubbles, p_{v} is assumed constant and p_{G} is expressed by the polytropic relation of index q: $p_{\mathrm{G}} = p_{\mathrm{G}_0}(R/R_0)^{3q}$, where p_{G_0} is the gas partial pressure at the reference radius R_0. Mass diffusion effects and other non-stationary phenomena are not, of course, included in the present theory. The determination of the polytropic index q requires the solution of the energy transfer problem across the bubble surface, as shown later in this Section. For now its value remains undetermined in the range from 1, in the isothermal limit, to γ, the ratio of the specific heats of the non-condensable gas in the bubbles, which corresponds to isentropic conditions.

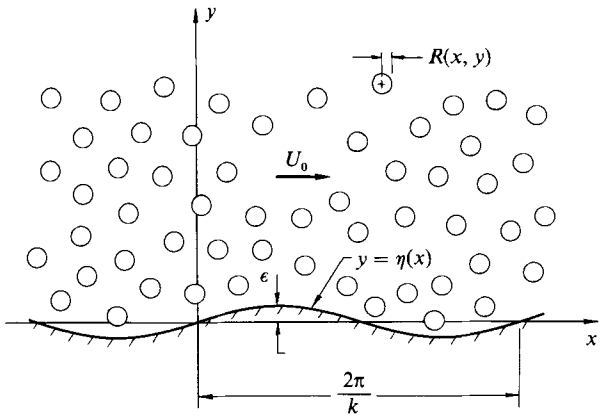

FIGURE 1. Schematic of a bubbly liquid flow over a wave-shaped surface.

Equations (1), (2) and (3), together with suitable boundary conditions, represent, in theory, a complete system of equations for $\boldsymbol{v}(\boldsymbol{x})$, $p(\boldsymbol{x})$ and $\tau(\boldsymbol{x})$. However, in practice their highly nonlinear nature requires further simplifications for a closed-form solution to be attained even for very simple flows.

3. Dynamics of bubbly flows over surfaces with slender profile

We consider first the problem of a two-dimensional inviscid flow of a bubbly liquid over a wave-shaped surface, as shown in figure 1. Let the wall profile be defined in complex notation by the equation: $\eta(x) = \epsilon \exp(ikx)$ with $k\epsilon \ll 1$ and let the subscript 0 indicate the unperturbed condition corresponding to $\epsilon = 0$. Then, if the flow velocity is U_0 and assuming, for simplicity, that all the bubbles have the same radius R_0, the undisturbed pressure in the liquid is:

$$p_0 = p_{G_0} + p_v - \frac{2S}{R_0}. \tag{4}$$

We limit our analysis to the case of relatively low void fraction $\alpha = \beta\tau/(1+\beta\tau)$ so that we can make use of first-order small-perturbation theory and write the velocity components as

$$\boldsymbol{v}(\boldsymbol{x}) = [U_0 + u(x, y)]\,\boldsymbol{i} + v(x, y)\boldsymbol{j},$$

with u and v much smaller than U_0. Here the pressure changes are not restricted to be small with respect to the equilibrium pressure because large perturbations of the pressure can result from the velocity field generated by the bubble volume changes, even though only small modifications of the fully wetted velocity field actually occur in low-void-fraction flows. Then (1), (2) and (3) reduce to

$$\frac{\partial u}{\partial x} + \frac{\partial v}{\partial y} = (1-\alpha_0)\,\beta U_0 \frac{4\pi}{3}\frac{\partial R^3}{\partial x}, \tag{5}$$

$$(1-\alpha_0)\,\rho U_0 \frac{\partial u}{\partial x} = -\frac{\partial p}{\partial x}, \tag{6}$$

$$(1-\alpha_0)\,\rho U_0 \frac{\partial v}{\partial x} = -\frac{\partial p}{\partial y}, \tag{7}$$

$$p = p_v + p_{G_0}\left(\frac{R_0}{R}\right)^{3q} - \frac{2S}{R} - \rho U_0^2\left[R\frac{\partial^2 R}{\partial x^2} + \frac{3}{2}\left(\frac{\partial R}{\partial x}\right)^2\right]. \tag{8}$$

Finally, eliminating u and v from (5), (6) and (7) and using (8), one obtains the following equation for $R(x, y)$:

$$\nabla^2\left\{\rho U_0^2\left[R\frac{\partial^2 R}{\partial x^2} + \frac{3}{2}\left(\frac{\partial R}{\partial x}\right)^2\right] + \frac{2S}{R} - p_{G_0}\left(\frac{R_0}{R}\right)^{3q}\right\} - \frac{\alpha_0(1-\alpha_0)\rho U_0^2}{R_0^3}\frac{\partial^2 R^3}{\partial x^2} = 0, \tag{9}$$

where ∇^2 is the two-dimensional Laplacian. Furthermore, the linearized kinematic condition at the wall: $v(x, y_w)/U_0 = \mathrm{d}\eta/\mathrm{d}x$ results in the following boundary condition for $R(x, y)$:

$$\frac{\partial}{\partial y}\left\{\rho U_0^2\left[R\frac{\partial^2 R}{\partial x^2} + \frac{3}{2}\left(\frac{\partial R}{\partial x}\right)^2\right] - p_{G_0}\left(\frac{R_0}{R}\right)^{3q} + \frac{2S}{R}\right\}_{y=y_w} = (1-\alpha_0)\rho U_0^2\frac{\mathrm{d}^2\eta}{\mathrm{d}x^2}, \tag{10}$$

where y_w is the ordinate of the wall profile corresponding to $\epsilon = 0$. In addition the solution is required to be periodic in x with wavenumber k.

The nonlinear equations (9) and (10) do not have any known analytical solution. In order to investigate their fundamental behaviour, we therefore examine the linearized form of these equations for small changes of the bubble radius: $R(x, y) = R_0[1 + \varphi(x, y)]$, where $\varphi(x, y) \ll 1$. Then, to the first order in φ:

$$\nabla^2\left(\frac{U_0^2}{\omega_B^2}\frac{\partial^2\varphi}{\partial x^2} + \varphi\right) - \frac{U_0^2}{c_m^2}\frac{\partial^2\varphi}{\partial x^2} = 0, \tag{11}$$

$$\frac{\partial}{\partial y}\left(\frac{U_0^2}{\omega_B^2}\frac{\partial^2\varphi}{\partial x^2} + \varphi\right)_{y=y_w} = \frac{(1-\alpha_0)U_0^2}{\omega_B^2 R_0^2}\frac{\mathrm{d}^2\eta}{\mathrm{d}x^2}, \tag{12}$$

where ω_B is the natural frequency of oscillation of a single bubble at isothermal conditions in an unbounded liquid (Plesset & Prosperetti 1977; Knapp *et al.* 1970):

$$\omega_B^2 = \frac{3p_{G_0}}{\rho R_0^2} - \frac{2S}{\rho R_0^3} \tag{13}$$

and

$$c_m^2 = \frac{\omega_B^2 R_0^2}{3\alpha_0(1-\alpha_0)} \tag{14}$$

is the low-frequency sound speed, i.e. in the absence of dispersive effects (van Wijngaarden, 1980). If the bubbles are in stable equilibrium in their mean or unperturbed state, then $3p_{G_0} > 2S/R_0$ and both ω_B and c_m are real.

When surface tension and vapour pressure are neglected (14) reduces to the well-known expression for the low-frequency sound speed of a homogeneous mixture (van Wijngaarden 1980). Similarly, in the reference frame moving with the flow free stream $U_0\partial/\partial x = -\partial/\partial t$, $U_0^2\partial^2/\partial x^2 = \partial^2/\partial t^2$ and (11) transforms into the familiar two-dimensional wave equation for the propagation of acoustical disturbances in a bubbly medium in the absence of energy dissipation (van Wijngaarden 1980):

$$\frac{1}{c_m^2}\frac{\partial^2\varphi}{\partial t^2} = \nabla^2\varphi + \frac{1}{\omega_B^2}\frac{\partial^2}{\partial t^2}\nabla^2\varphi. \tag{15}$$

The corresponding dispersion equation for waves of the form $\exp \mathrm{i}(\boldsymbol{h}\cdot\boldsymbol{x} - \omega t)$ is

$$\frac{1}{c_{m\omega}^2} = \frac{\boldsymbol{h}\cdot\boldsymbol{h}}{\omega^2} = \frac{1}{c_m^2}\left(\frac{\omega_B^2}{\omega_B^2 - \omega^2}\right), \tag{16}$$

where $c_{m\omega}$ is the speed of propagation of an harmonic disturbance of angular frequency ω. The present derivation of (11), however, has the advantage of explicitly formulating the boundary-value problem (9) and (10) which has to be addressed when the hypothesis of linearized bubble dynamics is relaxed.

The solution of (11) for the case of an unbounded bubbly flow over a wave-shaped wall is

$$\varphi(x,y) = \epsilon k(1-\alpha_0)\frac{U_0^2/R_0^2}{\omega_B^2 - k^2U_0^2}\frac{e^{ikx-Gky}}{G}; \quad y \geqslant 0. \tag{17}$$

Here G is the principal square root (with non-negative real and immaginary parts) of

$$G^2 = 1-M^2 = 1-\frac{U_0^2}{c_m^2}\left(\frac{\omega_B^2}{\omega_B^2 - k^2U_0^2}\right) \tag{18}$$

where $M = U_0/c_{m\omega}$ is the flow Mach number based on the sonic speed corresponding to the frequency $\omega = kU_0$ experienced by each bubble during its motion past the wavy surface. The other possible solution involving $\exp(ikx+Gky)$ has been eliminated since in the subsonic regime $(0 < M^2 < 1)\varphi(x,y)$ must be finite as $y \to +\infty$, and in the supersonic regimes ($M^2 > 1$ and $M^2 < 0$) no disturbance can propagate from the wall in the upstream direction. Therefore in the domain $y \geqslant 0$:

$$R(x,y) = R_0 + R_0\epsilon k(1-\alpha_0)\left(\frac{U_0^2/R_0^2}{\omega_B^2 - k^2U_0^2}\right)\frac{e^{ikx-Gky}}{G}, \tag{19}$$

$$u(x,y) = U_0 + U_0\epsilon k\frac{e^{ikx-Gky}}{G}, \tag{20}$$

$$v(x,y) = iU_0\epsilon k\, e^{ikx-Gky}, \tag{21}$$

$$p(x,y) = p_0 - (1-\alpha_0)\rho U_0^2\epsilon k\frac{e^{ikx-Gky}}{G}. \tag{22}$$

In the case of a wave-shaped channel of semiwidth b, the symmetry about the centreline $y = b$ provides the second boundary condition for the velocity: $v(x,b) = 0$ and the linearized solution of (11) takes the form

$$R(x,y) = R_0 + R_0\epsilon k(1-\alpha_0)\frac{U_0^2/R_0^2}{\omega_B^2 - k^2U_0^2}\left(\frac{\cosh Gk(b-y)}{\sinh Gkb}\right)\frac{e^{ikx}}{G}, \tag{23}$$

$$u(x,y) = U_0 + U_0\epsilon k\left(\frac{\cosh Gk(b-y)}{\sinh Gkb}\right)\frac{e^{ikx}}{G}, \tag{24}$$

$$v(x,y) = iU_0\epsilon k\frac{\sinh Gk(b-y)}{\sinh Gkb}e^{ikx}, \tag{25}$$

$$p(x,y) = p_0 - (1-\alpha_0)\rho U_0^2\epsilon k\left(\frac{\cosh Gk(b-y)}{\sinh Gkb}\right)\frac{e^{ikx}}{G}. \tag{26}$$

Energy dissipation in bubbly flows naturally originates from various sources such as viscosity, heat and mass transfer in the two phases and sound radiation from the bubbles. In particular, viscous effects occur owing to the interaction of the flow with the boundaries, to the relative velocity of the two phases, or as a consequence of the motion induced by the volume changes of the bubbles. In the further development of the theory of bubbly liquids over surfaces with slender profiles we only consider

the most important forms of damping which occur in the dynamics of the bubbles owing to thermal effects and to the viscosity and compressibility of the liquid. However, to the same order of approximations used here, the inclusion of the relative motion is indeed possible, as we intend to discuss in a later work where we consider the simultaneous solution of the fluid-dynamic equations for the two phases with the relevant interaction terms. The results of this analysis show that the relative motion slightly modifies the expression of the Mach-number parameter G^2 and generates, as expected, additional damping, but that its overall effects on the flow are usually quite small.

The effects of the liquid compressibility are included by introducing the speed of sound in the liquid $c = (\mathrm{d}p/\mathrm{d}\rho)^{\frac{1}{2}}$ and rewriting the continuity equation (1) as

$$\nabla \cdot \boldsymbol{v} = \frac{\beta}{1+\beta\tau}\frac{\mathrm{D}\tau}{\mathrm{D}t} - \frac{1}{\rho c^2}\frac{\mathrm{D}p}{\mathrm{D}t}. \tag{27}$$

In order to account for the viscous dissipation in the bubble dynamics, the Rayleigh-Plesset equation (3) is modified as indicated by Keller *et al.* (see Prosperetti 1984):

$$\left(1-\frac{\dot{R}}{c}\right)R\ddot{R} + \frac{3\dot{R}^2}{2}\left(1-\frac{\dot{R}}{3c}\right) = \left(1+\frac{\dot{R}}{c}\right)\frac{p_{\mathrm{R}}(t)+p(t+R/c)}{\rho} + \frac{R}{\rho c}\frac{\mathrm{d}p_{\mathrm{R}}(t)}{\mathrm{d}t}, \tag{28}$$

where $p_{\mathrm{R}}(t)$ is the liquid pressure at the bubble surface, related to the internal pressure p_{B} (assumed uniform) by

$$p_{\mathrm{B}}(t) = p_{\mathrm{R}}(t) + \frac{2S}{R} + 4\mu\frac{\dot{R}}{R}. \tag{29}$$

Here dots denote Lagrangian time derivatives and μ is the viscosity of the pure liquid. Linearization for small steady-state changes under the action of a periodic pressure perturbation $p(t) = p_0(1-\sigma\exp \mathrm{i}\omega t)$ leads to modelling each individual gas bubble as an harmonic oscillator:

$$\ddot{\varphi}(t) + 2\lambda\dot{\varphi}(t) + \omega_{\mathrm{B}\omega}^2\varphi(t) = \delta\sigma\,\mathrm{e}^{\mathrm{i}\omega t} \tag{30}$$

with internal pressure $p\mathrm{B}(t) = p_{\mathrm{B}_0}[1-\phi\varphi(t)]$, where

$$2\lambda = \frac{4\mu}{\rho R_0^2} + \frac{\omega^2 R_0}{c} + \frac{p_{\mathrm{B}_0}}{\rho\omega R_0^2}\,\mathrm{Im}(\phi), \tag{31}$$

$$\omega_{\mathrm{B}\omega}^2 = \mathrm{Re}\,(\phi)\frac{p_{\mathrm{B}_0}}{\rho R_0^2} - \frac{2S}{\rho R_0^3}, \tag{32}$$

$$\delta = \frac{p_0}{\rho R_0^2}\left(1-\mathrm{i}\frac{\omega R_0}{c}\right), \tag{33}$$

$$\phi = \frac{3\gamma\theta^2}{\theta[\theta+3(\gamma-1)A_-] - \mathrm{i}3(\gamma-1)(\theta A_+ - 2)} \tag{34}$$

$$A_\pm = \frac{\sinh\theta \pm \sin\theta}{\cosh\theta - \cos\theta}, \tag{35}$$

and $\theta = R_0(2\omega/\chi_{\mathrm{G}})^{\frac{1}{2}}$ is the ratio of the bubble radius to the bubble thermal diffusion length. The three terms of the effective damping coefficient λ respectively represent the contributions of the viscous, acoustic and thermal dissipation, while $\omega_{\mathrm{B}\omega}$ is the effective natural frequency of the oscillator when excited at frequency ω. Finally, the

complex parameters δ, ϕ and σ account for the magnitude ratio and phase difference between the related quantities. In particular, $\mathrm{Re}(\phi)/3$ can be interpreted as the effective polytropic exponent of the gas in the bubble and respectively tends to 1 and γ in the isothermal and isentropic limits for $\omega \to 0$ and $\omega \to +\infty$ (Prosperetti 1984).

By means of the Galilean transformation $\boldsymbol{x}' = \boldsymbol{x} - \boldsymbol{U}_0 t$ the above theory can be readily applied to the case of a bubbly flow over a wave-shaped surface. Here the frequency of the Lagrangian pressure change experienced by each bubble during its motion is: $\omega = kU_0$ and the following linearized approximations

$$\mathrm{D}/\mathrm{D}t \approx -U_0(\partial/\partial x), \quad \mathrm{D}^2/\mathrm{D}t^2 \approx U_0^2(\partial^2/\partial x^2)$$

can be used to express the Lagrangian derivatives in the Eulerian coordinates. Upon the assumption of a $2\pi/k$-periodic behaviour in the x-direction, damping can be incorporated in the theory for the linearized dynamics of bubbly flows over surfaces with slender profile. The previous approach leads to a generalized definition of the Mach-number parameter:

$$G^2 = 1 - M^2 = 1 - \frac{U_0^2}{c^2} - \frac{U_0^2}{c_{\mathrm{m}}^2}\left(\frac{\omega_{\mathrm{B}}^2(1 - \mathrm{i}kU_0 R_0/c)}{\omega_{\mathrm{B}\omega}^2 - k^2U_0^2 + \mathrm{i}2\lambda kU_0}\right), \tag{36}$$

which now becomes complex. It can be shown that $\mathrm{Im}(G^2) \geqslant 0$, thus, with the same convention as before, $\mathrm{Re}(G) \geqslant 0$ and $\mathrm{Im}(G) \geqslant 0$. Note that the effects due to the compressibility of the liquid are small for flow velocities $U_0 \ll c$. The formal expressions (19)–(26) for the solution for the flow quantities remain the same, except for (19) and (23) which now become

$$R(x, y) = R_0 + R_0 \epsilon k(1 - \alpha_0)\left(\frac{(1 - \mathrm{i}kU_0 R_0/c)\, U_0^2/R_0^2}{\omega_{\mathrm{B}\omega}^2 - k^2U_0^2 + \mathrm{i}2\lambda kU_0}\right)\frac{\mathrm{e}^{\mathrm{i}kx - Gky}}{G}, \tag{37}$$

$$R(x, y) = R_0 + R_0 \epsilon k(1 - \alpha_0)\frac{(1 - \mathrm{i}kU_0 R_0/c)\, U_0^2/R_0^2}{\omega_{\mathrm{B}\omega}^2 - k^2U_0^2 + \mathrm{i}2\lambda kU_0}\left(\frac{\cosh Gk(b - y)}{\sinh Gkb}\right)\frac{\mathrm{e}^{\mathrm{i}kx}}{G}. \tag{38}$$

The entire flow has therefore been determined in terms of the material properties of the phases, the geometry of the wall profile and of the assigned quantities: β, R_0, U_0 and p_0.

Owing to the linear nature of the problem, the above solution can readily be generalized to the case of surfaces with arbitrary slender boundaries. If the wall profile is denoted by $\eta(x)$ and $H(k)$ is the Fourier transform of $\eta(x)$ such that in complex notation

$$\eta(x) = \int_0^{+\infty} H(k)\, \mathrm{e}^{\mathrm{i}kx}\, \mathrm{d}k, \tag{39}$$

then the linearized solution $f(x, y)$ of (11) admits the following integral representation:

$$f(x, y) = \int_0^{+\infty} H(k) f_k(x, y, k)\, \mathrm{d}k, \tag{40}$$

where $f_k(x, y, k)$ is the corresponding wavy surface solution for given k and $\epsilon = 1$. Thus, for instance, the normalized bubble radius for the semi-infinite and channel flow cases is respectively expressed by

$$\varphi(x, y) = \int_0^{+\infty} H(k)\, k(1 - \alpha_0)\left(\frac{(1 - \mathrm{i}kU_0 R_0/c)\, U_0^2/R_0^2}{\omega_{\mathrm{B}\omega}^2 - k^2U_0^2 + \mathrm{i}2\lambda kU_0}\right)\frac{\mathrm{e}^{\mathrm{i}kx - Gky}}{G}\mathrm{d}k \tag{41}$$

and

$$\varphi(x,y) = \int_0^{+\infty} H(k)\, k(1-\alpha_0) \frac{(1-ikU_0 R_0/c)\, U_0^2/R_0^2}{\omega_{B\omega}^2 - k^2 U_0^2 + i2\lambda k U_0} \left(\frac{\cosh Gk(b-y)}{\sinh Gkb}\right) \frac{e^{ikx}}{G} dk, \quad (42)$$

where $G = G(k)$, $\omega_{B\omega} = \omega_{B\omega}(kU_0)$ and $\lambda = \lambda(kU_0)$. When no damping is present the integrands in the above equations have integrable square-root singularities corresponding to the sonic condition $k = k^*$ and to the bubble resonance condition $k = k_B$ (see §4). The latter also corresponds to the essential singularity due to the pole of G which appears in the argument of the exponential and hyperbolic functions. In (42) the additional singularities due to the finite well spacing $k = k_n$ behave as simple poles (see §4). In physical terms this reflects the fact that the absence of damping allows the bubble radius response to grow unbounded at resonance conditions. This difficulty is eliminated by the introduction of dissipative effects which limit the bubble response and generate a complex G^2, thus removing the singularity from the real k-axis.

4. Results for undamped bubble dynamics

We now examine the nature of the above solution considering first the undamped case. From (19) and (23) note that the bubble response is singular when:

(i) $G = 0$ and therefore the flow Mach number is equal to unity (sonic condition);

(ii) $(kU_0/\omega_B)^2 = 1$, namely the exciting frequency experienced by each bubble during its motion is equal to the natural frequency of an individual bubble in an infinite liquid (bubble resonance condition).

In addition, the channel flow is also singular when:

(iii) $Gkb = in\pi$; $n = 0, \pm 1, \pm 2, \ldots$.

The above conditions can be interpreted in two different ways according to whether the free-stream velocity or the wall wavenumber is assumed to be the independent variable. The former is the natural approach to the analysis of a given geometrical configuration at different flow regimes; the latter reflects the point of view used in deducing the solution for a more complex wall shape in terms of linear superposition of the different harmonic components of the wall profile.

The quantity G can be considered a function of the reduced frequency kU_0/ω_B and of the reciprocal of the dispersion parameter $\omega_B^2/k^2c_m^2$, when the wall geometry is fixed, or of the Mach number parameter U_0^2/c_m^2 when the flow velocity is constant. Consequently, (i) and (ii) can be used to deduce either the free-stream velocities or the wall wavenumbers which respectively correspond to sonic and bubble resonance conditions:

$$U_0^{*2} = \frac{\omega_B^2/k^2}{1+\omega_B^2/k^2c_m^2}; \quad k^{*2} = \frac{\omega_B^2}{U_0^2}\left(1-\frac{U_0^2}{c_m^2}\right), \quad (43)$$

$$U_{0B}^2 = \frac{\omega_B^2}{k^2}; \quad k_B^2 = \frac{\omega_B^2}{U_0^2}. \quad (44)$$

Similarly, for channel flow, conditions (iii) define the natural modes of the system, leading to infinite sequences of free-stream velocities or wall wavenumbers:

$$U_{0n}^2 = \frac{\omega^2}{k^2}\left(\frac{1+\omega_B^2/k^2c_m^2}{1+(n\pi/kb)^2}\right), \quad n = 0, \pm 1, \pm 2, \ldots, \quad (45)$$

$$k_n^2 = \frac{1}{2}\left\{k^{*2} - \frac{n^2\pi^2}{b^2} + \left[\left(k^{*2} - \frac{n^2\pi^2}{b^2}\right)^2 + 4\frac{n^2\pi^2}{b^2}\frac{\omega_B^2}{U_0^2}\right]^{\frac{1}{2}}\right\}, \quad n = 0, \pm 1, \pm 2, \ldots. \quad (46)$$

For large n these sequences respectively converge to the free-stream velocity and the wall wavenumber corresponding to the bubble resonance conditions. For small n the behaviour of these sequences is regulated by the values of $\omega_B^2/k^2c_m^2$ or U_0^2/c_m^2, which account for the relative importance of dispersion and compressibility effects in the flow. When these parameters are of order unity or larger, the lower terms of the above sequences will in general extend to values much smaller than the ones given by the bubble resonance condition (ii), thus indicating that the natural modes can occur at comparatively low frequency. On the other hand, when the reverse is the case, dispersion and compressibility effects are less significant, and all the terms of these sequences are contained in a small range below bubble resonance conditions. In this case all the natural modes of the system occur with a frequency only slightly lower than the bubble resonance frequency.

Clearly, the real and imaginary parts of G are respectively responsible for the attenuation and the speed of propagation of the wall-induced disturbances in the y-direction. The occurrence of bubble resonance and the presence of a finite sound speed divide the flow solutions in three different regimes, namely: subsonic ($0 < M^2 < 1$), supersonic ($M^2 > 1$) and super-resonant ($M^2 < 1$). As we shall see later, this has significant consequences for the behaviour of the flow. In the subsonic regime the wall disturbances can propagate in the upstream direction and the flow parameters resemble those of an incompressible flow, with the bubble response essentially in phase with the excitation. On the other hand, in the supersonic flows, where the perturbations cannot travel upstream, the typical delayed response of compressible flows appears and internal modes occur in the presence of suitable boundary conditions. Finally, in super-resonant flows the bubbles do not have time to respond as quickly as the excitation requires and the flow shows again the characteristics of incompressible flows, although the bubble response in this case tends to be out of phase with respect to the excitation.

The bubble response is maximum near bubble resonance conditions and, when damping is present, tends to be more localized in the proximity of the excitation source. The propagation of disturbances is also strongly affected by the dispersive nature of the sonic speed reflected in the frequency dependence of the Mach-number parameter G^2 in (18) and (36). In general the wall profile can excite the flow over a wide range of frequencies, depending on its shape and on the free-stream velocity. The spectral components of the wall profile excitation for which the flow is more nearly sonic tend to travel larger distances before being attenuated. Usually the sonic regime is close to the bubble resonance condition and its effects are therefore difficult to isolate, unless the parameters $\omega_B^2/k^2c_m^2$ or U_0^2/c_m^2 are of order unity. For this to happen relatively large flow velocities and void fractions are in general necessary, as discussed in §7.

Let us consider first the case of fixed wall geometry and variable free-stream velocity. Then the behaviour of the parameter G as a function of the reduced frequency is shown in figure 2 for some typical values of $\omega_B^2/k^2c_m^2$. Since G^2 is real (no damping) G is either real or purely imaginary. Note that all curves representing $\mathrm{Re}\,(G)$ start from unity at the origin and tend to move away from their horizontal asymptote $\mathrm{Re}\,(G) = 1$ (corresponding to the incompressible flow case) as the value of $\omega_B^2/k^2c_m^2$ increases. Also note that $\mathrm{Re}\,(G)$ vanishes in the supersonic regime between the sonic and bubble resonance conditions, where, on the other hand, $\mathrm{Im}\,(G) \neq 0$. The corresponding amplitudes of bubble radius oscillations at the wall ($kx = \frac{1}{4}\pi$ and $y = 0$) for the case of a semi-infinite flow with $k\epsilon/2\pi = 0.01$ are shown in figure 3, which also shows the migration of the sonic singularity from the bubble resonance

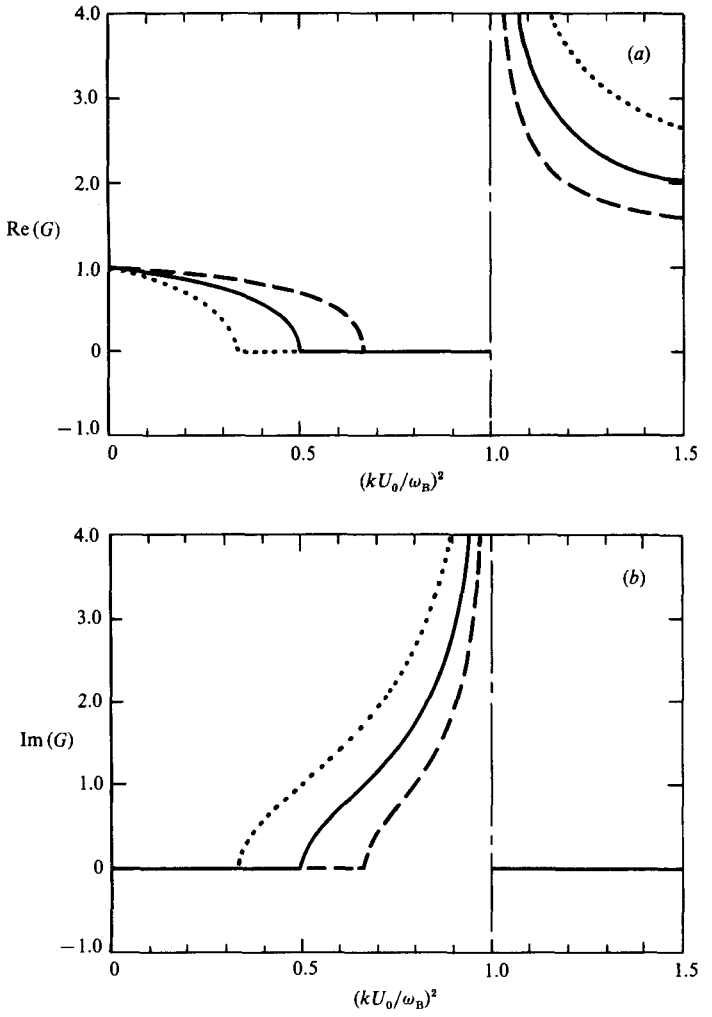

FIGURE 2. (*a*) Real and (*b*) imaginary parts of the parameter G versus the square of the reduced frequency $(kU_0/\omega_B)^2$ for different values of $\omega_B^2/k^2c_m^2 \approx 3\alpha_0/k^2R_0^2 = 0.5$ (-----), 1 (——) and 2 (·····).

condition towards the origin for increasing values of the parameter $\omega_B^2/k^2c_m^2$. Finally, the bubble radius response in the case of the channel flow is significantly different, as illustrated by figure 4, because of the presence of the additional resonances (iii) introduced by the finite spacing between the boundaries.

We assume next that the free-stream velocity is fixed and the wall wavenumber is allowed to vary. In this case the curves representing the parameter G as a function of the reduced frequency, now shown in figure 5, again display the tendency to move away from the horizontal asymptote $\mathrm{Re}\,(G) = 1$ as the value of the parameter U_0^2/c_m^2 increases. However, the value of G at the origin now depends on the free-stream velocity and can be either real, zero or imaginary according to whether the flow is respectively subsonic, sonic or supersonic. The normalized bubble radius response amplitudes at the wall ($kx = \frac{1}{4}\pi$ and $y = 0$) for the case of a semi-infinite flow with $k\epsilon/2\pi = 0.01$ are shown in figure 6. Here, as expected from the above considerations, when the free-stream velocity increases the sonic resonance moves

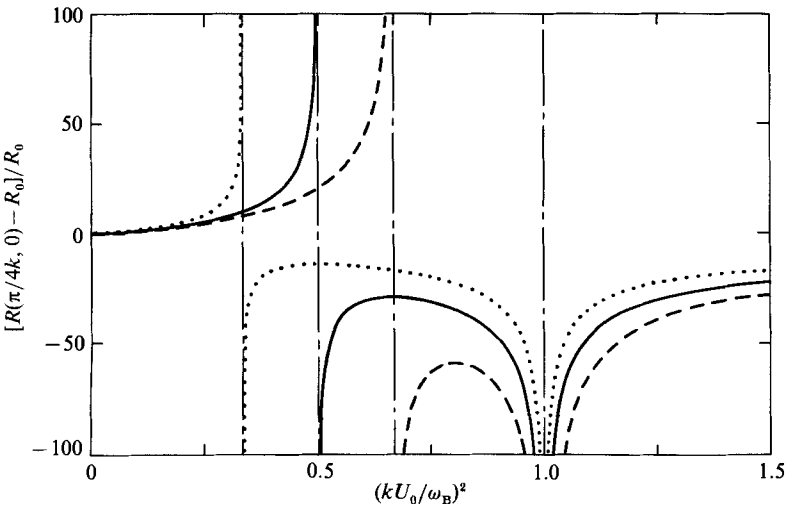

FIGURE 3. Response of a semi-infinite undamped bubbly flow over a wave-shaped wall as a function of the square of the reduced frequency $(kU_0/\omega_B)^2$ with $k\epsilon/2\pi = 0.01$. Normalized amplitudes of the bubble radius oscillations at the wall ($kx = \frac{1}{4}\pi$ and $y = 0$) are shown for different values of the parameter $\omega_B^2/k^2c_m^2 \approx 3\alpha_0/k^2R_0^2 = 0.5$ (-----), 1 (——) and 2 (·····).

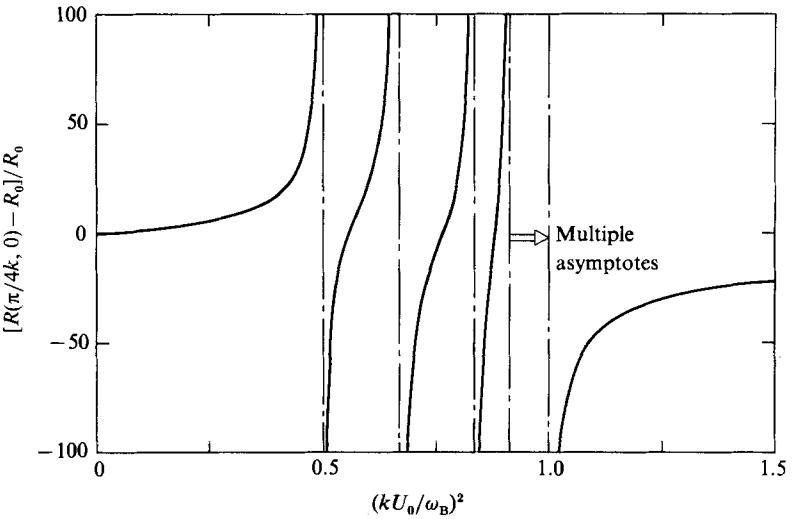

FIGURE 4. Response of an undamped bubbly flow in a symmetric wavy-wall channel as a function of the square of the reduced frequency $(kU_0/\omega_B)^2$ with $k\epsilon/2\pi = 0.01$. Normalized amplitudes of the bubble radius oscillations at the wall ($kx = \frac{1}{4}\pi$ and $y = 0$) are shown for $\omega_B^2/k^2c_m^2 \approx 3\alpha_0/k^2R_0^2 = 1$ and $kb = \pi$.

from the bubble resonance conditions to the origin and finally disappears for supersonic flows.

The parameter G also controls another important aspect of the flow, namely the penetration of wall-induced disturbances in the y-direction, which (19) and (23) show to be inversely proportional to $\mathrm{Re}\,(G)k$. In effect, when $\mathrm{Re}(G)$ is considerably larger than unity the response of the layer of bubbles near the wall essentially shields the rest of the mixture, with the result that the penetration of the disturbances induced by the wall is significantly reduced. On the other hand, as $\mathrm{Re}\,(G)$ approaches zero

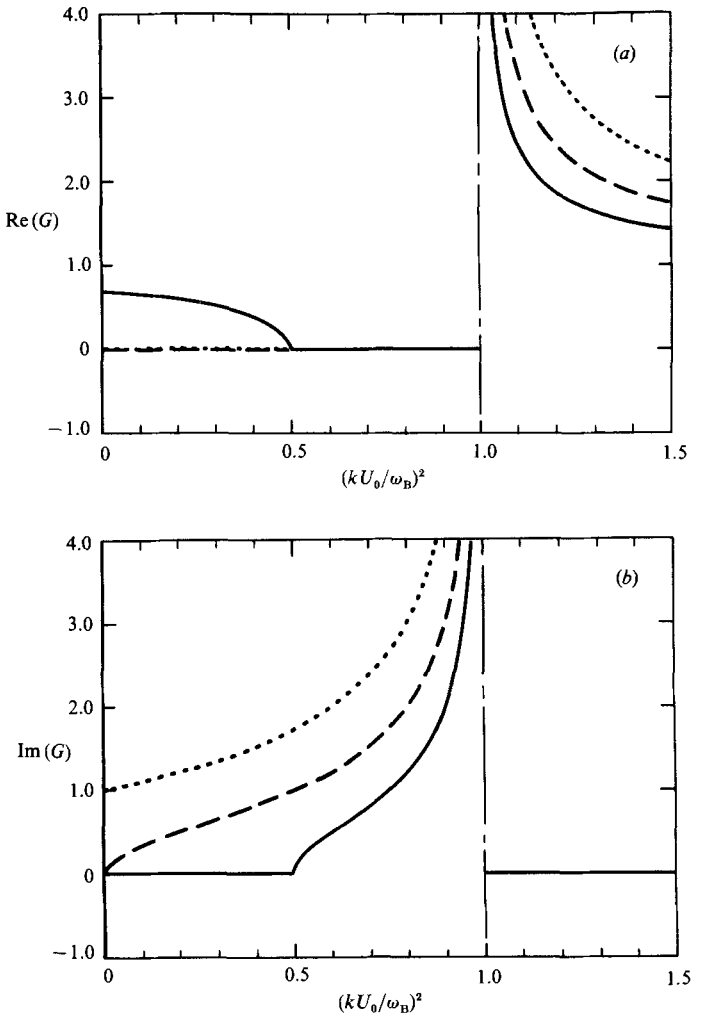

FIGURE 5. (*a*) Real and (*b*) imaginary parts of the parameter G versus the square of the reduced frequency $(kU_0/\omega_B)^2$ for different values of $U_0^2/c_m^2 \approx 3\alpha_0 U_0^2/\omega_B^2 R_0^2 = 0.5$ (——), 1 (- - - -) and 2.5 (·····).

near sonic conditions, the perturbations due to the wall tend to affect the whole flow.

5. Results with bubble damping

In general terms the introduction of energy dissipation in the bubble dynamics has the consequence of bounding the bubble response at the resonance condition, of providing smooth transitions between the various regimes and of eliminating higher-order internal modes. In the rest of this section we consider the case of air bubbles ($\gamma = 1.4$, $\chi_G = 0.0002$ m^2/s) in water ($\rho = 1000$ kg/m^3, $\mu = 0.001$ N s/m^2, $S = 0.0728$ N/m, $c = 1485$ m/s). The other relevant flow parameters are: $p_0 = 10^5$ Pa, $R_0 = 0.001$ m, $\epsilon = 0.001$ m and, when applicable, $k = 20\pi$ m^{-1}, $U_0 = 250$ m/s. Further comment on the dimensionless variables and practical values of both the dimensionless and dimensional variables is included at the end of §7.

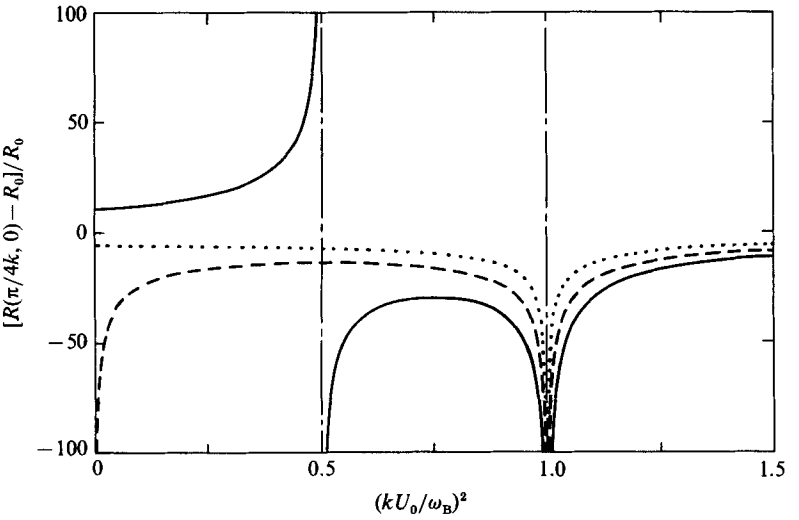

FIGURE 6. Response of a semi-infinite undamped bubbly flow over a wave-shaped wall as a function of the square of the reduced frequency $(kU_0/\omega_B)^2$ with $k\epsilon/2\pi = 0.01$. Normalized amplitudes of the bubble radius oscillations at the wall ($kx = \frac{1}{4}\pi$ and $y = 0$) are shown for different values of the parameter $U_0^2/c_m^2 \approx 3\alpha_0 U_0^2/\omega_B^2 R_0^2 = 0.5$ (——), 1 (-----) and 2.5 (·····).

In the damped case the effective bubble resonance frequency $\omega_{B\omega}(\omega)$, (32), is a function of the exciting frequency, $\omega = kU_0$, and extends from the value corresponding to isothermal conditions in the bubbles ($\omega = 0$ and $\phi = 3$), equal to the definition in the absence of damping, to the isentropic value reached in the limit for $\omega \to +\infty$. In what follows, normalization has been carried out with respect to the bubble resonance frequency ω_B defined as the solution of the equation: $\omega_B = \omega_{B\omega}(\omega_B)$. This choice has no special meaning, but preserves the occurrence of bubble resonance for $kU_0/\omega_B = 1$, with the advantage of making the plots for the damped case more readily comparable to the corresponding ones in the absence of damping.

We now examine the solution for the flow over wave-shaped surfaces with damped bubble dynamics. Since most of the phenomena manifest in the undamped solutions are still relevant, we shall limit ourselves to the illustration of the main differences introduced by the inclusion of dissipative effects. Let us again consider first the case of fixed wall geometry and variable free-stream velocity. The parameter $|G|$ in figure 7 (*a*) no longer goes to zero and infinity at sonic and bubble resonance conditions; instead it passes through a minimum and a maximum, which separate the various flow regimes. The different behaviour of the solution in the subsonic, supersonic and super-resonant regimes is now reflected in the relative importance of the real and imaginary parts of G, which change rapidly at the transition from one regime to the next, as shown in figure 7. In particular, the comparatively large value of Im (G) is related to the propagation of flow disturbances from the wall in the downstream direction at a relatively shallow angle, which is typical of the supersonic regime. On the other hand, the large value of Re (G) reflects the rapid attenuation of the flow disturbances propagating away from the wall, as happens in the subsonic and super-resonant cases. As expected, the flow response is no longer singular when energy dissipation is taken into account. The amplitudes of the bubble radius oscillation at the wall ($y = 0$) for a semi-infinite flow are shown in figure 8 and simply display a first maximum at sonic conditions and a second more pronounced one corresponding to

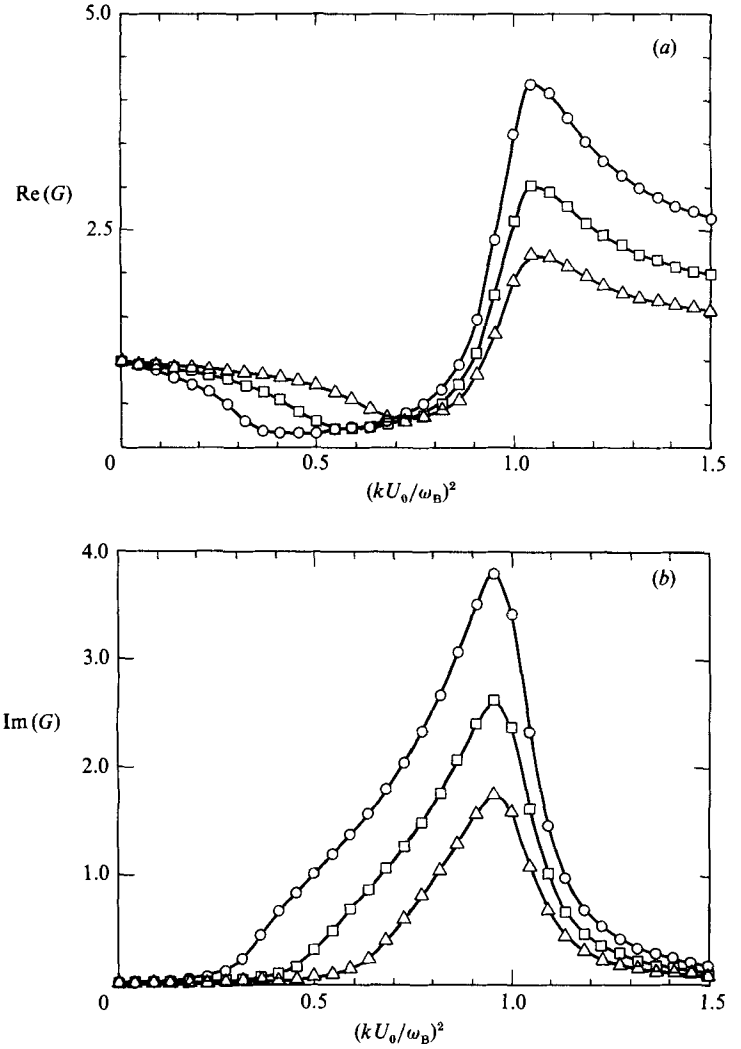

FIGURE 7. (*a*) and (*b*) imaginary part of the parameter G versus the square of the reduced frequency $(kU_0/\omega_B)^2$ for different values of $\omega_B^2/k^2c_m^2 \approx 3\alpha_0/k^2R_0^2 = 0.5$ (△), 1 (□) and 2 (○).

the bubble resonance. Similarly, in the bubble radius response of figure 9 for the channel flow case all but the lowest resonances due to the internal motion are virtually eliminated by the presence of dissipative effects. The same phenomena were manifest when the free-stream velocity is fixed and the wall wavenumber is allowed to vary.

In all cases, increasing the void fraction substantially decreases the amplitude of bubble growth. As mentioned in the introduction, this phenomenon has been observed experimentally by Arakeri & Shanmuganathan (1985) and by M. Billet (1986, personal communication). It has important consequences for cavitation damage and noise.

Clearly bubbly flows produce lifting forces on the boundaries when their shape determines a net vertical displacement of the flow. They also always produce surface drag even in the absence of viscous effects at the boundaries. This is another important consequence of the compressible nature of bubbly flows, which determines

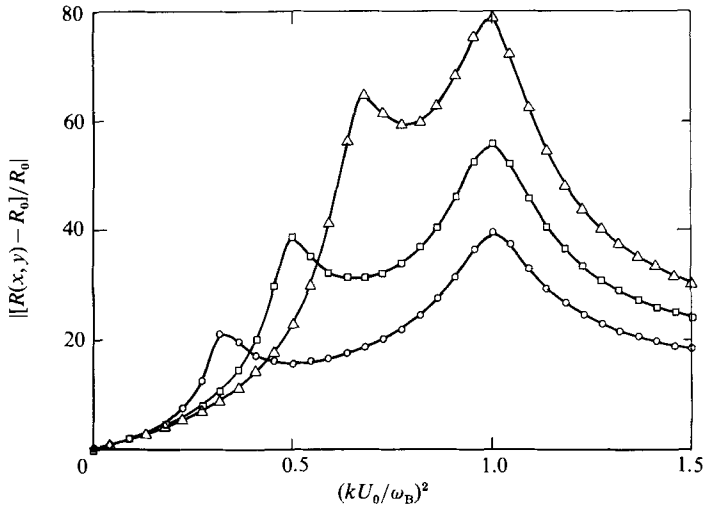

FIGURE 8. Response of a semi-infinite damped bubbly flow over a wave-shaped wall as a function of the square of the reduced frequency $(kU_0/\omega_B)^2$. Normalized amplitudes of the bubble radius oscillations at the wall ($y = 0$) are shown for different values of the parameter $\omega_B^2/k^2c_m^2 \approx 3\alpha_0/k^2R_0^2 = 0.5$ (△), 1 (□) and 2 (○).

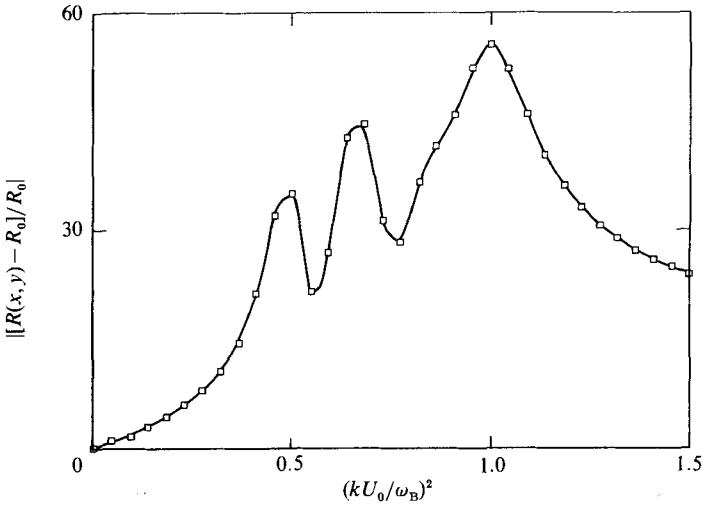

FIGURE 9. Response of a damped bubbly flow in a symmetric wavy-wall channel as a function of the square of the reduced frequency $(kU_0/\omega_B)^2$. Normalized amplitudes of the bubble radius oscillations at the wall ($y = 0$) are shown for $\omega_B^2/k^2c_m^2 \approx 3\alpha_0/k^2R_0^2 = 1$ and $kb = \pi$.

the transfer of energy from the flow velociety to the bubble motion under the influence of the perturbations induced by the wall. Indeed, as we shall see later, not all boundary shapes produce lift, but any deviation from a straight wall profile generates a drag force. As an example, the drag coefficient $C_D = 2D/\epsilon\rho U_0^2$ based on the drag per unit depth D on a wall wavelength in a semi-infinite bubbly flow is plotted in figure 10 for three values of the Mach-number parameter U_0^2/c_m^2. For increasing free-stream velocities the drag is initially zero, reaches a maximum near the sonic condition and finally tends to zero in the super-resonant regime where

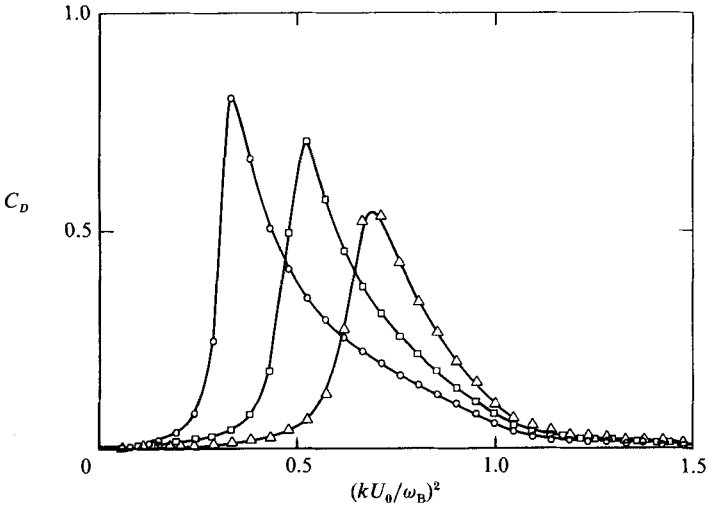

FIGURE 10. Drag coefficient $C_D = 2D/\epsilon\rho U_0^2$ in a semi-infinite damped bubbly flow over a wave-shaped wall as a function of the square of the reduced frequency $(kU_0/\omega_B)^2$ for different values of the parameter $\omega_B^2/k^2c_m^2 \approx 3\alpha_0/k^2R_0^2 = 0.5$ (△), 1 (□) and 2 (○).

compressibility effects asymptotically vanish. The lift on a wall wavelength in the same flow is identically zero, since no net vertical displacement of the flow is produced by a full period of the wall profile.

Significant analogies exist between the results shown here for the case of bubbly flows over slender profiles and the ones previously obtained for the linearized dynamics of clouds of bubbles (d'Agostino & Brennen 1983). In both flows the dispersive behaviour due to bubble dynamics effects is controlled by similar parameters, G^2 and λ^2, which depend on the bubble concentration and the excitation frequency. These parameters also determine the elliptic or hyperbolic nature of the solution, the penetration of external disturbances and the occurrence of the natural mode shapes and frequencies of the flow.

Finally, as a concluding remark, it is easily verified that the above theory reduces (as expected) to the first-order perturbation solutions for incompressible and homogeneous compressible flows in the limit for zero void fraction or free-stream velocity and zero wall wavenumber, respectively.

6. Results for a single, Gaussian-shaped bump

We now consider a semi-infinite bubbly flow over a slender surface with a Gaussian-shaped profile $\eta(x) = \epsilon \exp(-x^2/2a^2)$ of maximum height $\epsilon \ll a$. The Fourier transform, as defined by (39), is

$$H(k) = (2/\pi)^{\frac{1}{2}}\epsilon a \, \mathrm{e}^{-k^2a^2/2}.$$

As shown earlier, the solution for this flow is expressed by the inverse Fourier integrals (40). When dissipative effects are included the integrands have no singularities and are readily computed. It is convenient also in this case to define characteristic parameters whose values are related to the importance of sonic and bubble resonance effects. By analogy with the solution for a harmonic profile we can

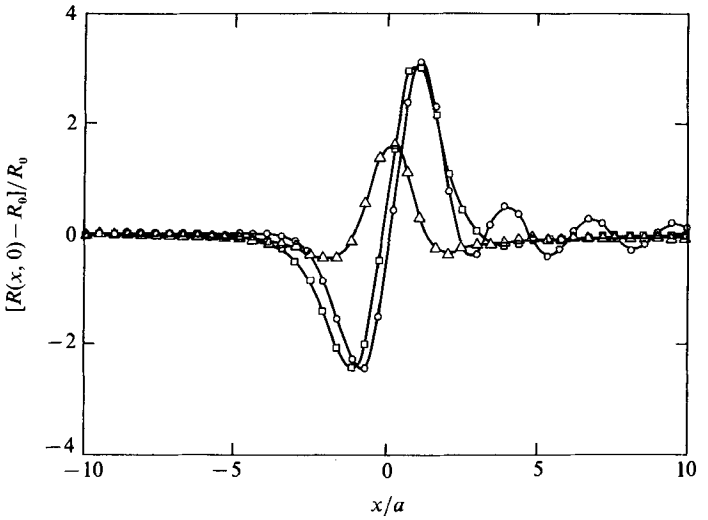

FIGURE 11. Response of a damped semi-infinite bubbly flow over a Gaussian-shaped profile as a function of the non-dimensional horizontal coordinate x/a. Normalized amplitudes of the bubble radius oscillations at the wall ($y = 0$) are shown for $\omega_B^2 a^2/\pi^2 c_m^2 = 1$ and for $(U_0\pi/a\omega_B)^2 = 0.5$ (△), 1 (□) and 2 (○).

anticipate that $2\pi/k$ will now be replaced by $2a$, and the relevant parameters in the case of a Gaussian bump are $\omega_B^2 a^2/\pi^2 c_m^2$ for dispersion effects and the square of the reduced frequency $(U_0\pi/a\omega_B)^2$ for the bubble resonance condition.

The bubble radius response at the wall ($y = 0$) is shown in figure 11 for $\omega_B^2 a^2/\pi^2 c_m^2 = 1$ and for three values of the square of the reduced frequency, $(U_0\pi/a\omega_B)^2$. Note that for the lower value of the reduced frequency the bubble radius response is essentially in phase with the expected behaviour of the pressure at the wall in the fully wetted flow case. Bubble inertial effects are only reflected in the small delay which makes the curve slightly asymmetric with respect to the plane $x = 0$. However, when $(U_0\pi/a\omega_B)^2 = 1$ bubble dynamic effects become more important and the bubbles no longer have the time to respond as in the previous case. The bubble radius simply goes through a minimum corresponding to the positive slope of the profile, followed by a maximum and a slow return to the unperturbed free-stream conditions. For the larger value of the reduced frequency the bubble response is further delayed and the bubbles are excited into damped oscillations which slowly subside further downstream.

The bubble radius response in the channel flow case is illustrated in figure 12 for $kb = \pi$, where the situation is modified by the presence of the internal flow modes of the system introduced by the finite spacing between the boundaries. For the lower value of the reduced frequency the behaviour is similar to the semi-infinite flow case. For higher values of $(U_0\pi/a\omega_B)^2$ this similarity is only restricted to the early stages of the bubble radius response. Later the internal flow modes of the system are excited and they variously interact to produce the more complex oscillatory behaviour of the downstream portion of the flow.

The propagation of wall-induced disturbances inside the semi-infinite flow over a Gaussian-shaped profile is illustrated in figure 13 which shows the bubble radius response at increasing distances from the wall: $y = 0$, $5a/\pi$ and $10a/\pi$. The values of the parameters $\omega_B^2 a^2/\pi^2 c_m^2 = 1$ and $(U_0\pi/a\omega_B)^2 = 1$ have been chosen in order to make

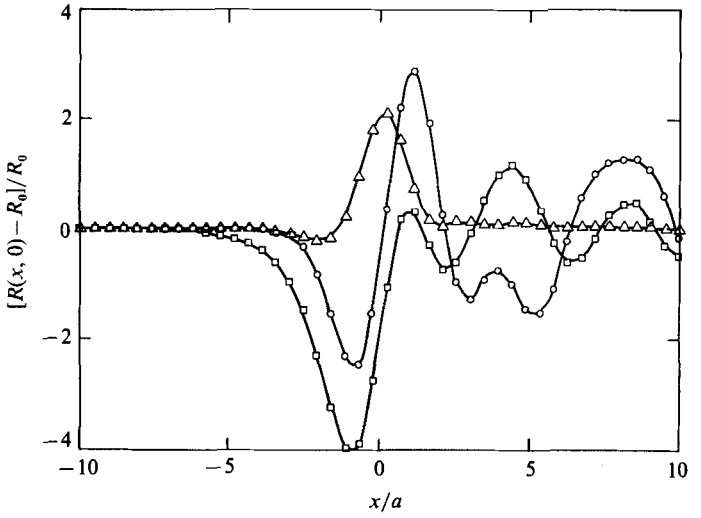

FIGURE 12. Response of a damped bubbly flow in a symmetric channel with Gaussian-shaped profile as a function of the non-dimensional horizontal coordinate x/a. Normalized amplitudes of the bubble radius oscillations at the wall ($y = 0$) are shown for $\omega_B^2 a^2/\pi^2 c_m^2 = 1$, $kb = \pi$ and for $(U_0\pi/a\omega_B)^2 = 0.5$ (△), 1 (□) and 2 (○).

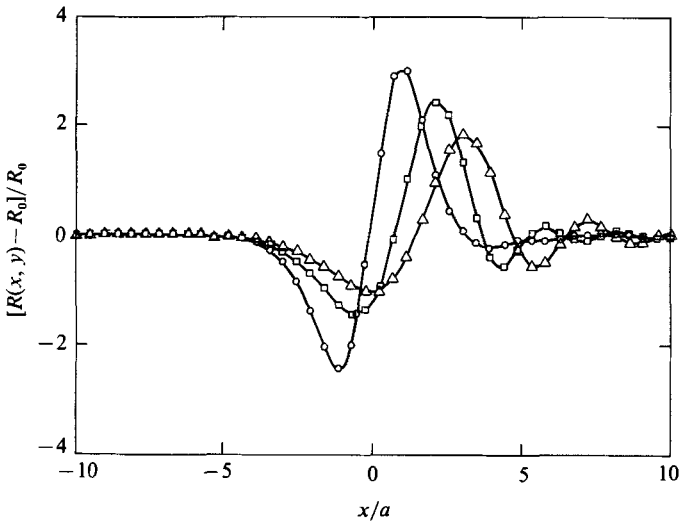

FIGURE 13. Response of a damped semi-infinite bubbly flow over a Gaussian-shaped profile as a function of the non-dimensional horizontal coordinate x/a. Normalized amplitudes of the bubble radius oscillations at various distances from the wall are shown for $\omega_B^2 a^2/\pi^2 c_m^2 = 1$, $kb = \pi$, $(U_0\pi/a\omega_B)^2 = 1$ and $y = 0$ (△), $5a/\pi$ (□) and $10a/\pi$(○).

both compressibility and bubble resonance effects important in this case. Hence the attenuation is relatively small, while the time delay of the bubble radius response at increasing distances from the wall is significant. Also note the inhibiting action that the proximity of the wall plays on the amplitude of the bubble radius oscillations in the downstream part of the flow.

The pressure distribution at the wall in the semi-infinite flow configuration, shown in figure 14 for $(\omega_B^2 a^2/\pi^2 c_m^2) = 1$ and for three values of the parameter

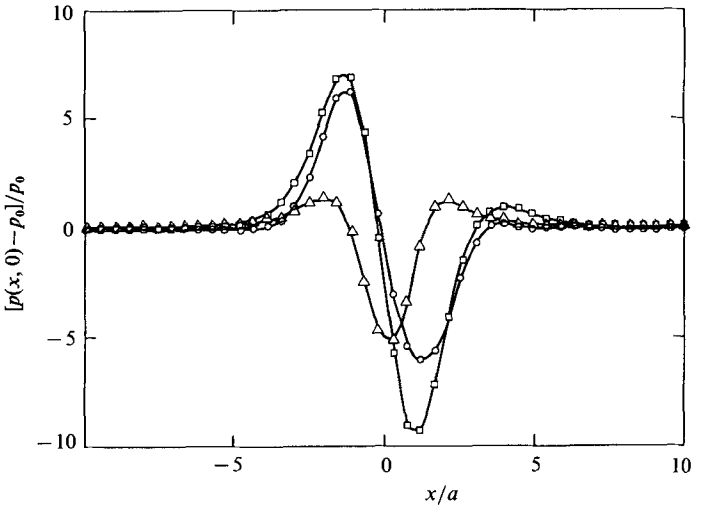

FIGURE 14. Response of a damped semi-infinite bubbly flow over a Gaussian-shaped profile as a function of the non-dimensional horizontal coordinate x/a. Normalized amplitudes of the pressure perturbation at the wall $y = 0$ are shown for $\omega_B^2 a^2/c_m^2 \pi^2 = 1$ and for three different values of the parameter $U_0^2/c_m^2 \approx 3\alpha_0 U_0^2/\omega_B^2 R_0^2 = 0.5$ (△), 1 (□) and 2 (○).

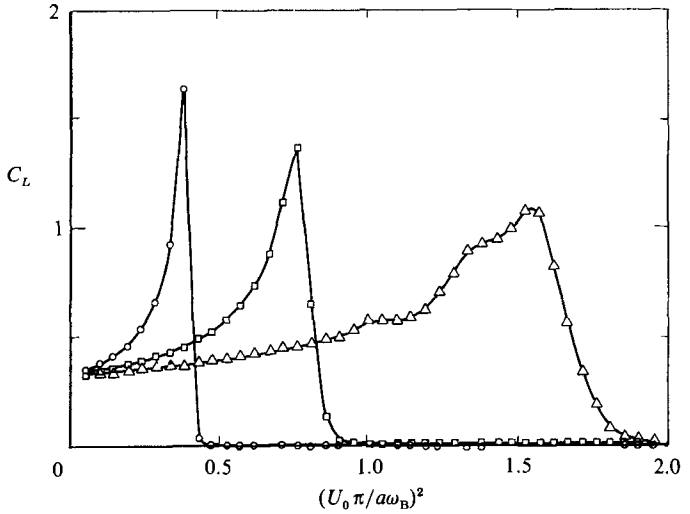

FIGURE 15. Lift coefficient $C_L = 2L/\epsilon\rho U_0^2$ in a semi-infinite damped bubbly flow over a Gaussian-shaped profile as a function of the reduced frequency parameter $(U_0\pi/a\omega_B)^2$ for three different values of the parameter $U_0^2/c_m^2 \approx 3\alpha_0 U_0^2/\omega_B^2 R_0^2 = 0.5$ (△), 1 (□) and 2 (○).

$U_0^2/c_m^2 \approx 3\alpha_0 U_0^2/\omega_B^2 R_0^2$, is similar to the bubble radius response, but exhibits a faster decay of the oscillations in the downstream region of the flow. Even a relatively small increase of the void fraction has a significant influence on the pressure distribution at the wall. In particular it is interesting to observe that increasing the void fraction values moves the minimum pressure point downstream; hence one would expect the laminar separation point to be similarly displaced downstream in real viscous flows. This consequence of the compressibility of the bubble mixture may well be responsible for the observed delay and even suppression of separation in travelling

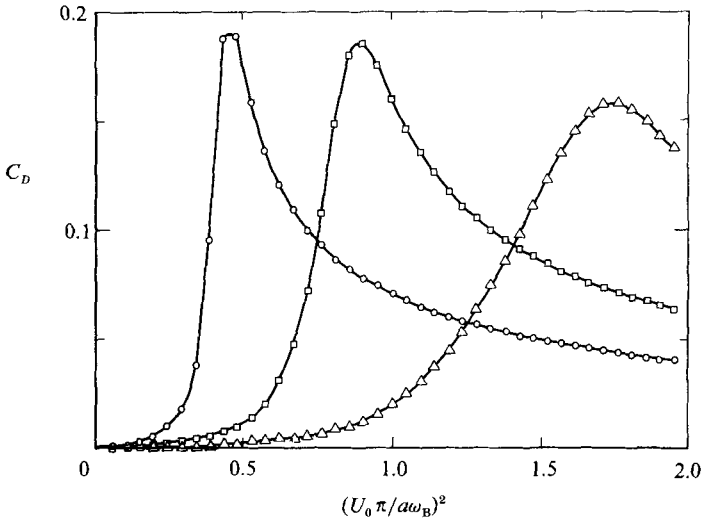

FIGURE 16. Drag coefficient $C_D = 2D/\epsilon\rho U_0^2$ in a semi-infinite damped bubbly flow over a Gaussian-shaped profile as a function of the reduced frequency parameter $(U_0\pi/a\omega_B)^2$ for three different values of the parameter $U_0^2/c_m^2 \approx 3\alpha_0 U_0^2/\omega_B^2 R_0^2 = 0.5$ (△), 1 (□) and 2 (○).

bubble cavitating flows over headforms with increased bubble content (Gates 1977). The lift and drag coefficients, $C_L = 2L/\epsilon\rho U_0^2$ and $C_D = 2D/\epsilon\rho U_0^2$, generated by the above pressure distributions are illustrated in figures 15 and 16 as a function of the reduced frequency parameter $(U_0\pi/a\omega_B)^2$ for three values of the parameter $U_0^2/c_m^2 \approx 3\alpha_0 U_0^2/\omega_B^2 R_0^2$. Here L and D are the lift and drag per unit depth on the wall profile. The behaviour of these coefficients is typical of compressible flows, with peaks near sonic conditions, followed by a rapid drop in the super-resonant regime, where only a thin layer of bubbles close to the boundary responds to the excitation.

7. Limitations

We now briefly examine the restrictions imposed to the previous theory by the various simplifying assumptions that have been made. Specifically we shall discuss the limitations due to the introduction of the continuum model of the flow, to the use of the linear perturbation approach in deriving the solution, to the neglect of the relative motion between the phases and of the local pressure perturbations in the neighbourhood of each individual bubble. In what follows we shall refer to the wavy-surface solution in the absence of damping, since it represents the most conservative case and the basis of the generalization to slender profiles of arbitrary shape.

The perturbation approach simply requires that $\varphi \ll 1$ in (17), a constraint that can be satisfied far from the sonic and bubble resonance conditions with proper choice of $k\epsilon$ and $U_0/\omega_B R_0$. This is probably the most restrictive limitation of the present analysis.

For the continuum approach to be valid, the two phases must be minutely dispersed with respect to the shortest characteristic length of the flow, here either the wall wave-length or the penetration of the wall disturbances in the y-direction. Hence the average bubble spacing $s = O(R_0/\alpha_0^{\frac{1}{3}})$ is required to satisfy the most restrictive of the two conditions: $ks \ll 1$ and $\mathrm{Re}\,(G)\,ks \ll 1$.

In order to estimate the error associated to the neglect of local pressure effects due

to the dynamic response of each individual bubble, we consider the pressure perturbation experienced by one bubble as a consequence of the growth or collapse of a neighbour:

$$\Delta p = \rho\left\{\frac{R}{s}\left[R\frac{\mathrm{D}^2R}{\mathrm{D}t^2}+2\left(\frac{\mathrm{D}R}{\mathrm{D}t}\right)^2\right]-\frac{R^4}{2s^4}\left(\frac{\mathrm{D}R}{\mathrm{D}t}\right)^2\right\}, \tag{47}$$

where $R = R_0(1+\varphi)$ is given by (19) or (23). To the same order of approximation used to develop the present analysis, comparison with the global pressure change expressed by (22) or (26) then shows that the local pressure perturbations are unimportant if

$$\alpha_0^{\frac{1}{3}}\left|\frac{k^2U_0^2/\omega_\mathrm{B}^2}{1-k^2U_0^2/\omega_\mathrm{B}^2}\right| \ll 1. \tag{48}$$

Far from the bubble resonance regime, this condition is generally satisfied in low void fraction flows.

Finally, in order to assess the error introduced by the neglect of the relative velocity between the two phases, let us consider the equation of motion for a bubble of negligible mass (Voinov 1973) with Stokes' viscous drag:

$$\frac{\mathrm{D}\boldsymbol{v}}{\mathrm{D}t}-\frac{1}{3}\frac{\mathrm{D}\boldsymbol{v}_\mathrm{B}}{\mathrm{D}t}+\frac{1}{R}\frac{\mathrm{D}R}{\mathrm{D}t}(\boldsymbol{v}-\boldsymbol{v}_\mathrm{B}) = \frac{2\nu}{R^2}(\boldsymbol{v}-\boldsymbol{v}_\mathrm{B}), \tag{49}$$

where $\boldsymbol{v}$ is the velocity of the liquid, $\boldsymbol{v}_\mathrm{B}$ is the velocity of the bubble and ν is the kinematic viscosity of the liquid. Linearizing as before and assuming for both the relative velocity $\boldsymbol{v}_\mathrm{r} = (\boldsymbol{v}-\boldsymbol{v}_\mathrm{B})$ and the velocity of the liquid a $2\pi/k$-periodic solution in the x-direction, one obtains

$$\left|\frac{\boldsymbol{v}_\mathrm{r}}{\boldsymbol{v}-\boldsymbol{v}_0}\right| = \frac{2}{[1+(6\nu/kR_0^2U_0)^2]^{\frac{1}{2}}} \ll 1. \tag{50}$$

Hence we expect that relative motion effects are unimportant when $kR_0^2U_0/\nu \ll 1$. Using the continuum hypothesis $kR_0 \ll 1$, this condition actually requires that $R_0U_0/\nu = O(1)$, which is already implicit in the assumption of Stokes' viscous drag. Thus the relative motion between the phases can be neglected as long as Stokes' expression correctly represents the drag on the bubbles. On the other hand, the above analysis does not allow us to assess to what extent this choice is justified. However, the more general simultaneous solution of the equations of motion for both phases, which we intend to discuss in a later publication, shows that the effect of relative motion is smaller than the above would suggest. It simply leads to a modified expression for the parameter G^2 involving a factor where unity is added to the void fraction multiplied by the square of the right-hand side of (50). The presence of the void fraction multiplier further reduces the estimate of the effect of relative motion.

We now briefly discuss the conditions for the effects of bubble dynamics and compressibility to become significant, showing that in general relatively high flow velocities and void fraction are required. As mentioned earlier, compressibility effects are expected to be important when the parameter $\omega_\mathrm{B}^2a^2/\pi^2c_\mathrm{m}^2 = 3\alpha_0a^2/R_0^2\pi^2$ is of order unity or greater, i.e. when: $\alpha_0 \geqslant O(R_0^2/a^2)$. For the validity of the present theory the typical dimension of the flow a must be much larger than the bubble size R_0, say $a/R_0 \geqslant 10$. Hence appreciable compressibility effects can take place when the void fraction is of the order of 0.01 or larger, a situation that can easily occur in practice. On the other hand, bubble dynamics effects become important when the reduced frequency parameter $(U_0\pi/a\omega_\mathrm{B})^2$ is of order unity or larger, i.e. when

$U_0 \geqslant O(a\omega_B)$. Consider, for example, the case of air bubbles in water. Usually the surface tension has little influence on the bubble natural frequency, thus, from (13), $\omega_B = O(p_0/\rho R_0^2)^{\frac{1}{2}}$, where for bubbles in equilibrium at about atmospheric pressure $(p_0/\rho)^{\frac{1}{2}} \approx 10$ m/s. Hence bubble dynamic effects are significant when $U_0 \geqslant O((a/R_0)(p_0/\rho)^{\frac{1}{2}})$, which requires the flow velocity to be of the order of 100 m/s or larger. Velocities of this magnitude are rare for objects moving inside liquids. The present linear theory therefore suggests that, unlike compressibility effects, important linear bubble dynamic phenomena are unlikely to be observed in most practical applications. However, the nonlinear response of the bubbles is characterized by much larger timescales and therefore bubble dynamic effects may still occur in practice at substantially lower speeds than indicated by the present linear analysis.

8. Conclusions

As anticipated in the introduction and confirmed by the present theory, the dynamics of the bubbles is strongly coupled through the pressure and velocity fields with the overall dynamics of the flow. The presence of the bubbles is responsible for the occurrence of bubble resonance phenomena and for the drastic modification of the sonic speed in the medium, which decreases and becomes dispersive (frequency dependent). The sonic and bubble resonance conditions lead in turn to the identification of three different flow regimes, here designated as subsonic, supersonic and super-resonant.

The inertial and resonance effects become important when the residence time of the bubbles is comparable with their typical response time: in the flows discussed here it is required that the reduced frequency parameter $(kU_0/\omega_B)^2$ for the flows with harmonic excitation of $(U_0\pi/a\omega_B)^2$ in the case of Gaussian excitation are of order unity. For this to happen relatively large flow velocities and bubble sizes are in general necessary.

Similarly, the effects related to the sonic regime become important and significantly separated from the bubble resonance condition when the reciprocal of the dispersion parameter $(\omega_B^2/k^2c_m^2$ for the flow over a wavy wall with fixed geometry, U_0^2/c_m^2 for the flow over a wavy wall with fixed free-stream velocity, or $\omega_B^2 a^2/\pi^2 c_m^2$ in the case of the Gaussian bump) is of order unity. For this to happen relatively large flow velocities and void fractions are in general necessary.

In the present work only the energy dissipation occurring in the dynamics of the bubbles has been considered, which represents the most important damping mechanism in bubbly flows. Additional contributions to the energy dissipation from the relative motion between the bubbles and the surrounding liquid can be included in the model, but their effects are expected to be small.

The results of this investigation reveal a number of qualitative effects which may be of importance in real cavitating flows around headforms or hydrofoils. First, an increase in the concentration of nuclei or bubbles causes a substantial reduction of the amplitude of growth of the bubbles as they are convected through a low-pressure region. We have already noted that such a phenomenon has been observed experimentally by Arakeri & Shanmuganathan (1985) and by Billet (1986, personal communication). This in turn could substantially reduce the acoustic noise or damage potential. Secondly, the compressibility of the flow produces a delay in the minimum pressure (and therefore in any laminar separation), a phenomenon noticed in the experiments of Gates (1977). This shift in the pressure distribution can also

generate drag, and similar changes in the lift coefficient could be anticipated for lifting surfaces. It remains to be seen whether this could help explain the well-known changes in lift and drag which result when cavitation is present.

The present theory has been derived under fairly restrictive simplifying assumptions involving the flow geometry and the linearization of both the velocity field and the bubble dynamics. Therefore, it is not expected to provide a quantitative description of the behaviour of steady bubbly flows over slender surfaces, except perhaps in the acoustical limit. Large bubble radius perturbations occur in most flows of practical interest; hence the most crucial limitation in the present paper is the linearization of the bubble dynamics, while the assumption of small velocity perturbations is likely to be more widely justified. If all the above linearizations were omitted only numerical solutions could be realistically attempted. However, if only the hypothesis of linear bubble dynamics is abandoned, the development of quasi-linear theories might be possible and would have a much broader applicability.

Even the very simple geometry of the flows considered here can nevertheless provide an introduction to the study of flows of great technical interest. Flows with similar geometry occur in many fields of applied hydrodynamics such as the study of propellers, lifting surfaces, pump blades, and yet general theories have only been developed in the fully wetted and supercavitating cases. In these flows the above theory might shed some light on the behaviour of the lift, drag and moment coefficients of the profiles, on the influence of the presence of the bubbles on boundary-layer development, on flow separation and other boundary viscous effects, on the problem of cavitation inception and its correlation to the nuclei number distribution of the liquid, and on the possible choice of more suitable parameters and laws for cavitation scaling. Finally, other more direct applications include the production and propagation of noise in cavitating flows.

The authors would like to thank Cecilia Lin for her help in drawing the pictures. This work was supported by the Naval Sea System Command General Hydromechanics Research Program Administered by the David Taylor Naval Ship Research and Development Center under Contract No. N00167-85-K-0165, by the Office of Naval Research under contract No. N0014-83-K-0506 and by a Fellowship for Technological Research administered by the North Atlantic Treaty Organization – Consiglio Nazionale delle Ricerche, Italy, Competition No. 215.15/11 of 11.5.1982. Their support is gratefully acknowledged. We also would like to thank our reviewers for their constructive comments and their contributions to the improvement of our work.

REFERENCES

ARAKERI, V. H. & ACOSTA, A. J. 1973 Viscous effects in the inception of cavitation on axisymmetric bodies. *Trans.* ASME I: *J. Fluids Engng* **95**, 519.

ARAKERI, V. H. & SHANMUGANATHAN, V. 1985 On the evidence for the effect of bubble interference on cavitation noise. *J. Fluid Mech.* **159**, 131–150.

CARSTENSEN, E. L. & FOLDY, L. L. 1947 Propagation of sound through a liquid containing bubbles. *J. Acoust. Soc. Am.* **19**, 481–501.

D'AGOSTINO, L. & BRENNEN, C. E. 1983 On the acoustical dynamics of bubble clouds, *ASME Cavitation and Multiphase Flow Forum*, pp. 72–75.

D'AGOSTINO, L., BRENNEN, C. E. & ACOSTA, A. J. 1984 On the linearized dynamics of two-dimensional bubbly flows over wave-shaped surfaces. *ASME Cavitation and Multiphase Flow Forum*, pp. 8–13.

FOLDY, L. L. 1945 The multiple scattering of waves. *Phys. Rev.* **67**, 107–119.

FOX, S. E., CURLEY, S. R. & LARSON, G. S. 1955 Phase velocity and absorption measurements in water containing air bubbles. *J. Acoust. Soc. Am.* **27**, 534–539.

GATES, E. M. 1977 The influence of free stream turbulence, free stream nuclei population and a drag reducing polymer on cavitation inception on two axisymmetric bodies, Ph.D. thesis, Calif. Inst. of Tech.

KNAPP, R. T., DAILY, J. W. & HAMMIT, F. G. 1970 *Cavitation*. McGraw Hill.

MACPHERSON, J. D. 1957 The effect of gas bubbles on sound propagation in water. *Proc. Phys. Soc. Lond.* **70 B**, 85–92.

MUIR, T. F. & EICHHORN, R. 1963 Compressible flow of an air–water mixture through a vertical two-dimensional converging–diverging nozzle. *Proc. Heat Transfer. Fluid Mech. Inst., Stanford.* Stanford University Press.

NOORDZIJ L. 1973 Shock waves in mixtures of liquids and air bubbles. Doctoral thesis, Technische Hogeschool, Twente, Netherlands.

NOORDZIJ L. & VAN WIJNGAÄRDEN, L. 1974 Relaxation effects, caused by relative motion, on shock waves in gas-bubble/liquid mixtures. *J. Fluid Mech.* **66**, 115–143.

PLESSET, M. S. & PROSPERETTI, A. 1977 Bubble dynamics and cavitation. *Ann. Rev. Fluid. Mech.* **9**, 145–185.

PROSPERETTI, A. 1984 Bubble phenomena in sound fields: part one. *Ultrasonics* March 1984, 69–78.

SILBERMAN, E. 1957 Sound velocity and attenuation in bubbly mixtures measured in standing wave tubes. *J. Acoust. Soc. Am.* **18**, 925–933.

TANGREN, R. F., DODGE, C. H. & SEIFERT, H. S. 1949 Compressibility effects in two-phase flows. *J. Appl. Phys.* **20**, 637–645.

VOINOV, O. V. 1973 Force acting on a sphere in an inhomogeneous flow of an ideal incompressible fluid. Plenum. (Transl. from *Z. Prikl. Mekh. i Tekh. Fiz.* **4**, 182–184, July–August 1973.)

WIJNGAARDEN, L. VAN 1964 On the collective collapse of a large number of gas bubbles in water. In *Proc. 11th Intl Congr. Appl. Mech.*, pp. 854–861. Springer.

WIJNGAARDEN, L., VAN 1968 On the equations of motion of mixtures of liquid and gas bubbles. *J. Fluid Mech.* **33**, 465–474.

WIJNGAARDEN, L. VAN 1972 One dimensional flow of liquids containing small gas bubbles *Ann. Rev. Fluid. Mech.* **4**, 369–396.

WIJNGAARDEN, L. VAN 1980 Sound and Shock Waves in B. bubbly Liquids. In *Cavitation and Inhomogeneities in Underwater Acoustics*, pp. 127–140. Springer.

WIJNGAARDEN, L. VAN 1983 Waves in gas–liquid flows In *Theory of Dispersed Multiphase Flow*, pp. 251–269, Academic.